Modeling the Impact of Behavior Changes on the Spread of Pandemic Influenza

Sara Y. Del Valle, Susan M. Mniszewski, and James M. Hyman

Abstract We use mathematical models to assess the impact of behavioral changes in response to an emerging epidemic. Evaluating the quantitative and qualitative impact of public health interventions on the spread of infectious diseases is a crucial public health objective. The recent avian influenza (H5N1) outbreaks and the 2009 H1N1 pandemic have raised significant global concerns about the emergence of a deadly influenza virus causing a pandemic of catastrophic proportions. Mitigation strategies based on behavior changes are some of the only options available in the early stages of an emerging epidemic when vaccines are unlikely to be available and there are only limited stockpiles of antiviral medications. Mathematical models that capture these behavior changes can quantify the relative impact of different mitigation strategies, such as closing schools, in slowing the spread of an infectious disease. Including behavior changes in mathematical models increases complexity and is often left out of the analysis. We present a simple differential equation model which allows for people changing their behavior to decrease their probability of infection. We also describe a large-scale agent-based model that can be used to analyze the impact of isolation scenarios such as school closures and fear-based home isolation during a pandemic. The agent-based model captures realistic individual-level mixing patterns and coordinated reactive changes in human behavior in order to better predict the transmission dynamics of an epidemic. Both models confirm that changes in behavior can be effective in reducing the spread of disease. For example, our model predicts that if school closures are implemented for the

S.Y. Del Valle (✉) • S.M. Mniszewski
Los Alamos National Laboratory, West Jemez Road, Los Alamos, NM 87545, USA
e-mail: sdelvall@lanl.gov; smm@lanl.gov

J.M. Hyman
Tulane University, St Charles Avenue, New Orleans, LA, USA
e-mail: mhyman@tulane.edu

P. Manfredi and A. d'Onofrio (eds.), *Modeling the Interplay Between Human Behavior and the Spread of Infectious Diseases*, DOI 10.1007/978-1-4614-5474-8_4,

duration of the pandemic, the clinical attack rate could be reduced by more than 50%. We also verify that when interventions are stopped too soon, a second wave of infection can occur.

1 Introduction

Pandemics are global epidemics and are often associated with a high morbidity and mortality burden. There have been three pandemic influenza outbreaks in the 20th history: the Spanish flu (1918–19), the Asian flu (1957–58), and the Hong Kong flu (1968–69) [32]. The 1918–1919 influenza pandemic (known as the Spanish flu) was the most devastating in recent history, where at least 20 million died [30]. In the United States, about 675,000 lives were lost to the Spanish flu with an estimated mean case fatality rate of 2% [52]. This case fatality rate is an order of magnitude larger than the case fatality rates observed in seasonal flu epidemics in normal years. Recurrent outbreaks of H5N1 around the world and the most recent pandemic (H1N1) 2009 suggest that a deadly pandemic is eminent.

Nearly half of the world's population resides in urban areas [50]. Air travel connects these urban centers in a global network where a new influenza strain can spread around the world in a few weeks, as recently experienced with pandemic (H1N1) 2009. In addition, influenza's short incubation period and the lack of a universal vaccine can increase the spread of influenza, posing a significant global challenge to public health officials. Mathematical models can help in meeting this challenge, if the model includes the most significant properties of the transmission dynamics. In particular, the model most include how people change their behavior in response to an epidemic threat.

Evidence suggests that in the presence of a deadly disease and lack of pharmaceutical interventions, people will change their behavior to avoid infection [15, 19, 42]. Recent studies have evaluated the impact that non-pharmaceutical interventions, such as school closures, social distancing, and travel restrictions, could have on the spread of the next influenza pandemic [13, 14, 21, 24]. However, none of these studies have incorporated intentional changes in individual behavior, such as avoiding gatherings, increasing hygiene, or staying home. Furthermore, these studies have assumed that these non-pharmaceutical interventions would remain in effect for the duration of the pandemic. Typically, people resume their normal behaviors due to lack of resources or as the perceived risk declines [27]. Recent studies on the impact of basic public health measures implemented during the 1918 pandemic [6, 27] indicate that non-pharmaceutical interventions did not last for the duration of the pandemic.

Mathematical models for the spread of infectious diseases have been extensively used to gain insights into the transmission dynamics of infectious diseases. Several approaches have been used for these studies including simple compartmental models [31, 44], network models [35], and agent-based models [18, 24, 34, 48].

These models have provided new insights on important issues such as the effects of drug resistance [5, 46], treatment [34, 40], vaccination [3, 45], non-pharmaceutical interventions [11, 15] and on the overall dynamics of infectious diseases [28].

Diseases often spread through person-to-person contacts; therefore, realistic mixing patterns can be crucial to accurately predicting the path and severity of the disease [16]. The course of an epidemic through a population is determined by the interactions among individuals and the process of transmitting a pathogen is a stochastic (random) process based on the length of time the individuals are in contact with each other and the strength of the contact. Agent-based models can capture this realistic contact structure and allow the simulation to explore how contact networks and different demographic characteristics affect disease transmission.

Several studies have shown the importance of population structure when modeling disease spread [20], but only a few studies have incorporated realistic mixing populations [18, 24]. The accurate representation of population heterogeneity is one of the greatest challenges of epidemic modeling. While substantial progress has been made over the years with the introduction of different mixing functions [29] and mixing matrices [2] for compartmental models, they are still far from achieving a good approximation to real world scenarios. In recent years, new approaches that incorporate more realistic contact structures have been developed to allow for nonrandom interactions among populations [4, 22, 48, 54]. For example, Zaric [54] compared random and nonrandom mixing patterns for network epidemic models and showed that different mixing assumptions led to different epidemic outcomes. In particular, they found that random mixing generally results in a greater number of new infections than nonrandom mixing. Similarly, Bansal et al. [4] used several real and simulated datasets of human contact networks to analyze their impact on disease spread. They concluded that homogeneous-mixing models are appropriate for host populations that are nearly homogeneous. However, network models are more appropriate to better capture and predict disease spread through heterogeneous host populations. Furthermore, Fukś et al. [22] used an agent-based model of Southern and Central Ontario to investigate the spatial correlations of disease spread. They concluded that spatial correlations were difficult to destroy if neighborhood sizes were inhomogeneous. Finally, Stroud et al. [48] showed a strong correlation between local demographic characteristics and pandemic severity. This study used an agent-based model of Southern California with a heterogeneously mixing population and concluded that the average household size in a census tract was strongly correlated with the clinical attack rate.

Here, we use a simple mathematical model to show how behavioral changes can be easily introduced into epidemiological models. In addition, we use a large-scale agent-based model to assess the potential impact of temporary and permanent behavioral changes including school closures in containing a pandemic influenza and analyze how these changes affect the contact structure and transmission dynamics.

2 Methods

We will consider two approaches to incorporate behavior changes in a mathematical model. We first describe a simple system of five ordinary differential equations (ODEs) to describe disease dynamics based on the Kermack–McKendrick susceptible-infected-recovered model (SIR) [31]. We extended this model by using the approaches introduced in Del Valle et al. (2005) [15]. The second approach is based on a stochastic agent-based model, object-oriented platform for people in infectious epidemics (OPPIE). This is an extension of the Los Alamos Epidemic Simulation System (EpiSimS) [16, 18, 48] and includes dynamic behavior changes.

2.1 Ordinary Differential Equation Model

In our ODE model, the population is divided into two subgroups: a group that does not change its behavior or has *normal* behavior (subscript n) and a group that modifies its *behavior* in response to an outbreak (subscript b). People move back and forth between the two groups (reducing susceptibility or infectivity) depending on the behavior adopted. Individuals in each activity group are characterized by their epidemiological status: susceptible, S_n and S_b and infectious individuals, I_n and I_b; the transfers are shown diagrammatically in Fig. 4. Because we are primarily interested in the effectiveness of changes in behavior for a single outbreak, we use a closed system with no migration in or out of the population, and births and natural deaths are not included in the model.

We define t_0 as the beginning of the epidemic. Movement of individuals between the two groups depends upon disease incidence in the population. It is assumed that a certain fraction of the population will change their behavior to protect themselves against infection or reduce their chances of spreading the disease. Let $\varphi_{S_b} S_n$ and $\varphi_{I_b} I_n$ be the transfer rates from the S_n and I_n classes to the S_b and I_b classes, respectively, and $\varphi_{S_n} S_b$ and $\varphi_{I_n} I_b$ be the transfer rates from the S_b, and I_b classes to the S_n and I_n classes, respectively. The rate coefficients are modeled by step functions given by:

$$\varphi_i = \begin{cases} 0, t < \tau \\ c_i, \ \tau < t < \tau_{max} \\ 0 \ t > \tau_{max} \end{cases}$$

for i $= S_n, I_n, S_b$, and I_b, where the parameter c is a positive constant that determines the rate of movement and τ is the time that determines when the new behavior is adopted.

Using the transfer diagrams in Fig. 1, we obtain the following system of differential equations:

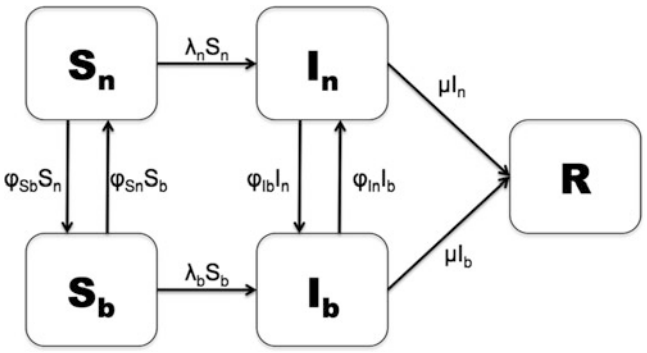

Fig. 1 Schematic relationship between people who adopt a new behavior in response to an epidemic and people who do not change their behavior. The arrows that connect the boxed groups represent movement of individuals from one group to an adjacent one. Susceptible individuals (S_n or S_b) can become infected (I_n or I_b) at rates λ_n or λ_b; infected individuals recover at a rate μ; and people change their behavior based on the transfer rates φ_{S_b}, φ_{I_b}, φ_{S_n}, or φ_{I_n}

$$
\begin{aligned}
\frac{dS_n}{dt} &= -(\varphi_{S_b} + \lambda_n)S_n + \varphi_{S_n} S_b \\
\frac{dI_n}{dt} &= -(\varphi_{I_b} + \mu)I_n + \varphi_{I_n} I_b + \lambda_n S_n \\
\frac{dS_b}{dt} &= -(\varphi_{S_n} + \lambda_b)S_b + \varphi_{S_b} S_n \\
\frac{dI_b}{dt} &= -(\varphi_{I_n} + \mu)I_b + \varphi_{I_b} I_n + \lambda S_b \\
\frac{dR}{dt} &= \mu(I_n + I_b)
\end{aligned} \tag{1}
$$

where λ_n (for normal behavior) and λ_b (for modified behavior) are the forces of infection. λ_n and λ_b incorporate the probability of transmission per contact, β, the reduced number of contacts because of symptomatic infection, θ, and $1 - \eta_j$ (j = s or i), which accounts for the effectiveness of the behavior in reducing either susceptibility (η_s) or infectivity (η_i). β is defined as the susceptibility of the population multiplied by the infectivity of the disease multiplied by the average number of contacts an individual has per day. The forces of infection for both groups are shown by:

$$
\begin{aligned}
\lambda_n &= \beta \left[\left(\frac{\theta I_n}{\rho} \right) + (1 - \eta_i) \left(\frac{\theta I_b}{\rho} \right) \right] \\
\lambda_b &= \beta \left[(1 - \eta_s) \left(\frac{\theta I_n}{\rho} \right) + (1 - \eta_i)(1 - \eta_s) \left(\frac{\theta I_b}{\rho} \right) \right]
\end{aligned} \tag{2}
$$

where $\rho = N - (1-\theta)(I_n + I_b)$ and N is the total population $(S_n + S_b + I_n + I_b + R)$. In the forces of infection, η_i is incorporated into the $\theta I_b/\rho$ infectious fractions because individuals in the I_b class have adopted a new behavior and η_s is incorporated into the infectious fractions in λ_b because individuals in the susceptible class (S_b) have also adopted a new behavior. These forces of infection and appropriate initial conditions complete our model formulation.

2.2 The Agent-Based Model

The OPPIE simulation platform is an agent-based model that combines the demographic-based population of a region, a network of specific business and home locations, and the movement of individuals between locations with daily itineraries. We simulated the spread of an influenza epidemic using a synthetic population constructed to statistically match the 2000 US Census population demographics of Southern California at the census tract level. There are 20 million individuals living in six million households, with an additional one million locations representing actual schools, businesses, shops, and social recreation addresses. This synthetic population only represents individuals reported as household residents; thus, visiting tourists, guests in hotels, and travelers in airports are not explicitly included.

Each individual has a schedule of activities based on the National Household Transportation Survey (NHTS) [37]. A schedule specifies the type of activity, the starting and ending time, and the location of each assigned activity. There are six types of activities: *home*, *work*, *shopping*, *social recreation*, *school*, and *other*. The time, duration, and location of activities determine which individuals mix together at the same location at the same time, which is relevant for airborne transmission.

Each location is geographically located using the Dun & Bradstreet commercial database. Each building is subdivided based on the number of activities available at that location. There are one or more buildings per activity that are further subdivided into rooms or mixing places. Schools have classrooms, workplaces have workrooms or offices, and shopping malls have shops. Typical room sizes can be specified; for example, for workplaces the mean workgroup size varies by standard industry classification (SIC) code. The number of rooms in each building is computed by dividing the peak occupancy by the appropriate mixing group size. We used two data sources to estimate the mean workgroup by SIC including a study on employment density [53] and a study on commercial building usage from the Department of Energy [36]. Based on these two data sources workgroup sizes range from 3.1 for transportation workers to 25.4 for health service workers. The average workgroup size over all types of work is 15.3. For the analyses presented here, the average mixing group sizes are 8.5 at a school, 4.4 at a shop, and 3.5 at a social recreation venue.

2.2.1 Disease Progression Model

Airborne diseases spread primarily from person to person during close proximity through contact, sneezing, coughing, or via fomites. In OPPIE, an opportunity for disease spread between two individuals occurs when they occupy a mixing location together. Whether or not a susceptible individual becomes infected is based on how long they co-occupy within a mixing place, the presence of infectious individuals, a high-level description of the activity they are engaged in, and their age.

A location represents a street address, and a room or mixing place represents a specific place where people have face-to-face interactions. When an infectious person is in one of these mixing locations with a susceptible person for some time, we estimate a probability of disease transmission, which depends on the variables identified above.

A susceptible person j has a dimensionless susceptibility multiplier S_j and an infectious person i has an infectious multiplier I_i. The probability that the susceptible individual j becomes infected during an activity is computed as:

$$P_j = 1 - e^{-\sum_i T S_j I_i t_{ij}} \tag{3}$$

where T is the average transmissibility per unit time, t_{ij} is the duration of contact, and the sum extends over all infectious people that occupied the room with individual j.

Disease progression of the epidemic is modeled as a Markov chain consisting of five main epidemiological stages: uninfected, latent (non-infectious), incubation (partially infectious), infectious, and recovered. Infected individuals start in the incubation stage and remain there for a period of between 0 and 0.5 days, 0.5 or 1.0 day, before transitioning to the symptomatic or recovered stages, respectively. The average incubation time is 1.9 days and average duration of the symptomatic stage is 4.1 [34]. The disease model assumes that 50% of adults and seniors, 75% of students, and 80% of preschoolers will stay home within 12 hours of the onset of influenza symptoms. These people can then transmit disease only to household members or visitors. Based on previous studies [34], 33.3% of infections are assumed to be subclinical. Individuals in the subclinical stage are only half as infectious as those in the symptomatic stages and continue their normal activities as if they were not infected. The infection rate for children is assumed to be double than for adults. All scenarios were analyzed for the same set of transmission parameters where the population was initially seeded with 100 people infected, all in the incubation stage.

2.2.2 Baseline Assumptions

The Homeland Security Council released the National Strategy for Pandemic Influenza for the United States, which suggests that the emergence of a new influenza virus could have a clinical disease attack rate of 30% in the overall

population [49]. Based on this attack rate, we constructed a baseline scenario under the assumption of no specific intervention to contain the pandemic and an infection attack rate of 45% with a clinical attack rate of 30%.

2.2.3 School Closure Assumptions

Protecting children during an influenza pandemic is important since illness rates are typically highest among school-aged children [38]. Closing schools limits students' contacts and has the potential to block paths of spread between families and neighborhoods [1]. Several studies have analyzed the impact of school closures [8,21,24]; however, these studies only investigated the impact of sustaining a school closed during the entire epidemic. School closures in OPPIE are implemented as a general closure of selected activity locations. Based on the Center for Disease Control and Prevention pandemic guidelines [9], closures in OPPIE follow a steplike function and are specified with a start and stop time; the activity to close; and a single location or a fraction of all locations of the specified activity type that will be closed. During the time a closure is in effect, anyone whose activity schedule would have taken them to one of the closed locations will stay home during that time instead. Scheduled after-school activities are not affected by a school closure.

2.2.4 Fear-Based Home Isolation Assumptions

Fear-based home isolation consists of people staying home as a reaction to an epidemic crisis. Some of these people may be considered the "worried well". The news of increasing numbers of people becoming ill, or seeing friends and family fall ill, is strong motivation to avoid potential infectious situations. Surprisingly, none of the recent studies on pandemic influenza have incorporated the impact of this type of behavioral change. We assume that people isolate due to fear at a level that follows the pattern of the epidemic [6, 27]. This is implemented with a specification of start, peak, and end times with corresponding fractions of the population that will be isolating at those times, along with a minimum and maximum contiguous duration per individual. We assume that people who choose to stay home will only self-isolate for 7–14 days at a time. People isolate on an individual basis, not on a household basis, so there might be households in which some members of the family are isolating due to fear and others are going about their normal activities. Fear-based home isolation begins when a percentage of the population is symptomatic (e.g., 0.1%). The number of people self-isolating increases linearly until reaching a maximum near the epidemic peak day. After this day, the stay-home rate begins to drop linearly with time, until no fear-based home isolation is occurring by a selected end day.

2.2.5 Strain-Specific Vaccine Assumptions

Currently, vaccine manufactures need an estimated 5–8 months to develop a strain-specific egg-based vaccine [47]. Based on seasonal influenza vaccine production, we estimate U.S. production at four million doses per week; thus, we assume that a limited number of vaccines, enough to cover 0.67% of the population per week, will be available five months after the emergence of pandemic influenza. We further assume that two doses of pandemic vaccine are required to attain an immune response of 80% seropositivity after 42 days from the first dose [33]. Those who are vaccinated and become sick are only 20% as infectious as those who become sick without the vaccine. In all of the scenarios where a strain-specific vaccine is considered, the strain-specific vaccine is distributed as soon as it becomes available. Vaccine is distributed to households at random until supplies run out; 95% of the selected household members are vaccinated, and 5% either refuse treatment or cannot be found.

3 Results

Here we show how we use both models to analyze the impact that behavioral changes may have on disease transmission. In particular, we look at the impact of some generic behavior for the ODE type model and school closures and fear-based home isolation for the agent-based model.

3.1 Ordinary Differential Equation Results

We recognize that large agent-based simulations may require significant infrastructure such as high performance computing; therefore, we analyze a simple ODE model and show how behavioral changes can modify disease dynamics.

We used the model presented in Sect. 2.1 and analyzed the impact that temporary behavioral changes (e.g., school closures) may have on the spread of an airborne infection. We use a population of 10,000 people and start the simulation with one infected person. We assume that some generic behavior is implemented for two weeks (14 days) starting on day 25. Furthermore, we assume that the behavior reduces susceptibility and infectivity by 50%, that is, $\eta_s = 0.5$ and $\eta_i = 0.5$. In addition, we assume that θ, a reduction in contact rates due to symptomatic infection, is 0.8. Finally, we assume that β, the probability of infection, is 0.4. Figure 2 shows the epidemic curves as a function of time for S_n, S_b, I_n, and I_b. Not that as people change their behavior, the disease spread slows down. Since behavioral changes are only temporary and do not provide a permanent cure to the disease, the virus eventually infects everyone in the population (due to homogeneous assumptions).

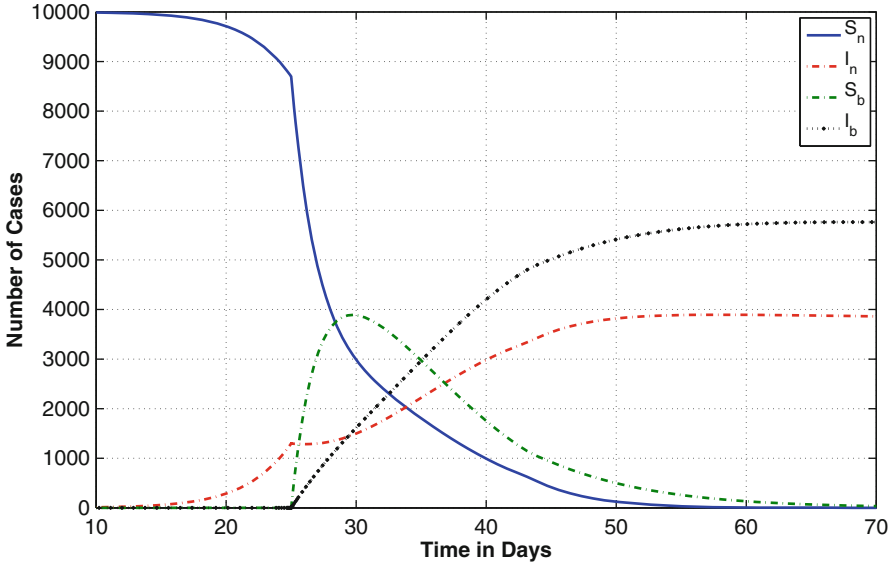

Fig. 2 *Epidemic curves* for various groups within the population including S_n, S_b, I_n, and I_b. Note that as the changes in behavior are implemented (starting on day 25), the disease transmission slows down

3.2 Agent-Based Model Results

3.2.1 Baseline Simulation

The baseline scenario was constructed with no specific intervention to contain the pandemic and an infection attack rate of 45% with a clinical attack rate of 30%. A key quantity in epidemiology is the basic reproduction number (denoted by R_0) defined as the average number of secondary cases generated by a primary infectious case in a completely susceptible population [2]. Hence, the R_0 concept only applies to the case of newly emergent infectious agents or situations when the disease in question has not been observed in a given population for a long period of time, so that the population is essentially entirely susceptible. This concept applies to most pandemics, particularly to the influenza pandemic of 1918 for which the mean R_0 has been estimated to range from 1.5 to 5.4, depending on the specific location and pandemic wave considered [10]. For consistency with historical pandemics [23,34], we considered a moderately severe pandemic strain with an R_0 of 1.8, which is in agreement with the transmissibility baseline assumed in other modeling studies [21, 23, 34]. OPPIE tracks who infects whom and so the value of R_0 was calculated using the average number of secondary infections generated by the index cases.

Table 1 Results for the baseline and various durations of 100% school closures

	Baseline	5-month 1st wave	5-month 2nd wave	8-month 1st wave	8-month 2nd wave	11-month
Clinical attack rate (%)	30.6	14.1	12	14.1	8.5	14.1
Pandemic duration (days)	150[a]	190[b]	350[a]	190[b]	465[a]	300[a]
Mortality per 100,000	614	279	240	282	164	281
Population vaccinated (%)	0	0	15.7	0	25.5	13.1

[a]When the number of newly infected cases has reached zero
[b]When the number of newly infected people has reached its lowest point before ramping up again

3.2.2 School Closures and Vaccination

School closures can provide an effective way to reduce the spread of the epidemic. We assumed that schools close when 0.1% of the population is symptomatic (day 33), and they remain closed for 5, 8, or 11 months. Table 1 shows that in the absence of any interventions, the model predicts a 30.6% clinical attack rate and 614 influenza-related deaths per 100,000 persons in the population. However, our results show that if schools remain closed for 11 months, the clinical and mortality attack rate would be reduced by more than 50%.

In Fig. 3, we show the symptomatic percentage of the population as a function of time for the baseline and for 100% school closures for 5, 8, and 11 months. School closures might be relaxed after 5 and 8 months, if a strain-specific vaccine becomes available. In the 5 month school closure scenario, schools reopen on day 183 when 0.0007% (14,238 people) is infected; in the 8 month scenario, schools reopen on day 273 when 0.00003% (721 people) of the population is infected. However, if schools close for the duration of the pandemic (in this case 11 months), the disease dies out and no second wave is generated. Unlike previous studies that have shown that the benefit provided by school closures is maintained after schools reopen [25], our simulation results show that, given the limited number of vaccine doses, if schools reopen too early a new infection wave appears, resulting in an increased number of new cases. Nevertheless, even in the presence of infection waves, the overall clinical attack rate for these three scenarios of school closures is lower than the baseline. Although school closures prolong the epidemic due to the reduction in the number of contacts, they benefit society by spreading the number of hospitalizations over two waves, which is crucial in order to maintain health-care services operational. Our results show that school closures for the duration of the pandemic (up to 11 months) are the most effective strategy in containing the pandemic and reducing morbidity and mortality. Furthermore, the 11 month strategy also reduces the number of vaccinations needed to contain the pandemic.

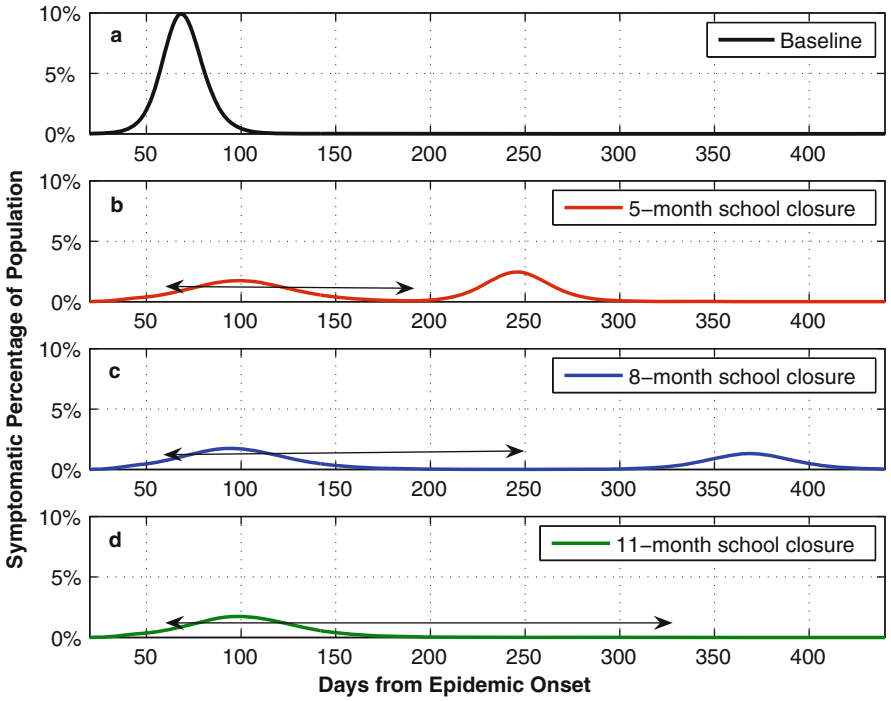

Fig. 3 Symptomatic percentage of the population as a function of time for the baseline scenario and three school closure scenarios. (**a**) shows the simulated epidemic curve for the baseline scenario, (**b**) shows the results for a 5-month closure scenario, (**c**) shows the results for an 8-month closure scenario, and (**d**) shows the results for the 11-month 100% closure scenario. The *arrows* indicate the time when school closures are in effect. Note that as the interventions are relaxed (schools reopen), new infection waves can appear (panels (**b**) and (**c**))

3.2.3 Fear-Based Home Isolation and Vaccination

In Table 2, we illustrate the simulation results for various levels of fear-based home isolation. When the percentage of population self-isolating at home, due to fear, is 15%, the clinical attack rate and death rate decrease, but the percentage of infections generated at home increases. When the number of people self-isolating is greater than 50%, the epidemic is partitioned into two infection waves and the number of infected people increases.

Figure 4 shows a comparison of the effective reproduction number and the epidemic dynamics for the baseline and 50% fear-based home isolation. $R_{\text{effective}}$ captures the effects of public health interventions and depletion of the susceptible population as the epidemic progresses. Note that $R_{\text{effective}}$ drops below 1 when the number of susceptibles declines, but as fear-based home isolation is relaxed and the social contact networks return to normal, $R_{\text{effective}}$ increases. In general, we observe that even if a small fraction of the population reduces their interactions for a

Table 2 Results for the baseline and various levels of fear-based home isolation

	Baseline	15%	30%	50% 1st wave	50% 2nd wave	60% 1st wave	60% 2nd wave
Clinical attack rate (%)	30.6	25.9	20.5	13	9.6	7.6	18.2
Pandemic duration (days)	150[a]	211[a]	300[a]	184[b]	372[a]	161[b]	340[a]
Mortality per 100,000	614	517	411	251	199	150	364
Population vaccinated (%)	0	2.8	5.9	0	17.8	0	13.3
Infections generated at home (%)	58.4	62.2	65.8	65	65	62.9	62.9

[a]When the number of newly infected cases has reached zero
[b]When the number of newly infected people has reached its lowest point before ramping up again

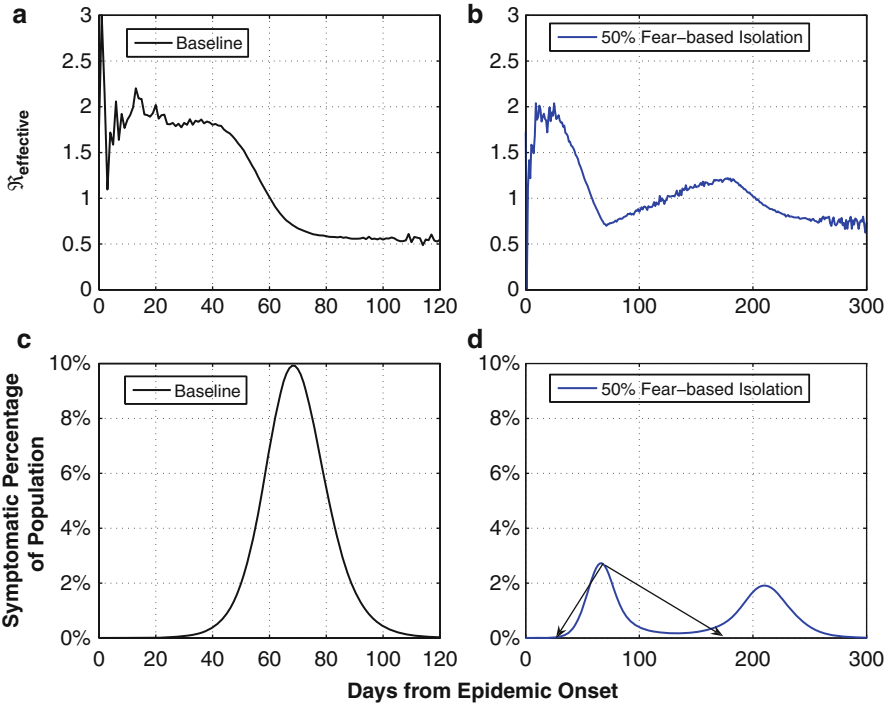

Fig. 4 Epidemic dynamics for the baseline and 50% fear-based home isolation for 5-months. (**a**) and (**b**) show the effective reproduction number as a function of time for the baseline and 50% fear-based home isolation, respectively. (**c**) and (**d**) show the symptomatic percentage of the population for the baseline and the 50% fear-based home isolation scenario

week or two, morbidity and mortality can be reduced, but the epidemic is prolonged; however, temporal compliance of large fractions of people can create susceptible populations, resulting in waves of infection [6, 27, 41].

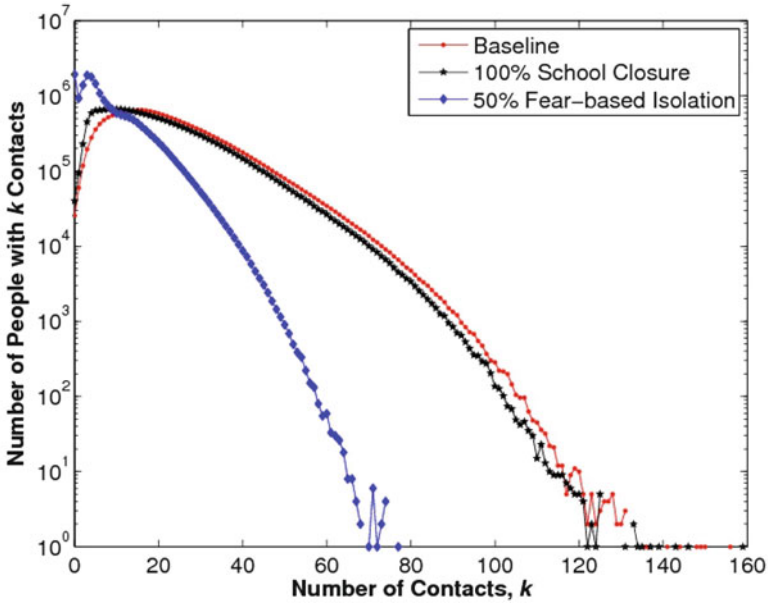

Fig. 5 Degree distribution of the population in Southern California under three different scenarios for a typical day. On average, each individual has 22.5, 19.9, and 8 contacts per day for the baseline, 100% school closure scenario (5-month), and 50% fear-based home isolation scenario, respectively

3.2.4 Impact on Social Contact Network

Population mixing information is key to provide good approximation on the path of the disease and devise effective intervention strategies. Here, we apply tools from social network epidemiology [35,39,43] to study how changes in behavior affect the contact network and, as a result, disease transmission. The social contact network emerges from the simulation as individuals move through their daily activities and come into and out of contact in rooms [11]. We extracted the degree distribution of the social contact structure in the absence of disease during a random day for the baseline, 100% school closure scenario, and at the peak of the 50% fear-based home isolation scenario. Figure 5 depicts the population distribution in Southern California under the three scenarios for a typical day. On average, each individual has 22.5, 19.9, and 8 contacts per day for the baseline, 100% school closure scenario, and 50% fear-based home isolation scenario, respectively. We observe that the average number of contacts per day decreased for the school closure and fear-based home isolation scenarios when compared to the baseline. Note that the average number of people contacted per person can provide an estimate of how many people can potentially acquire infection from one index case. Furthermore, we found that closing schools would be less effective in breaking the social contact network than fear-based home isolation. This finding might be due to the fact that school closures

imply partial home isolation; individuals affected by this intervention still perform other scheduled activities, except for school-related activities. While fear-based home isolation assumes that people affected by this intervention are completely cut off from the rest of the population, our results show that reactive changes in population contact rates can have a dramatic impact on the overall contact structure.

4 Discussion

We used two types of modeling approaches to show that coordinated or reactive behavioral modifications can have a significant effect not only in reducing disease burden but also on the qualitative dynamics of influenza transmission. Although vaccination would be the best means for controlling influenza, a strain-specific vaccine will not be available until 5–8 months after the emergence of a new pandemic influenza and current production capabilities are insufficient to cope with demand. Antivirals share important features that could make them useful during a pandemic [34], although most countries do not have enough antivirals stockpiled and current distribution strategies may not allow for rapid dissemination of drugs. Behavioral modifications have the potential to slow down the spread of the pandemic in the absence of pharmaceutical interventions.

We argue that models that use social contact networks and human behavior are better able to capture the dynamics of infectious-disease transmission than models that ignore human behavior or use homogeneous mixing. We showed how easy one can incorporate behavioral changes in traditional ODE epidemiological models and how simple assumptions can change the dynamics of disease transmission.

The emergent degree distribution of the baseline social network is in agreement with contact patterns observed in small convenience samples [17, 51]. Although we cannot compare the emergent contact patterns in the presence of school closures and fear-based home isolation due to lack of data, our simulation results are useful in providing estimates of the effects of behavioral changes on disease burden and gain insights into potential qualitative effects on the transmission dynamics (e.g., multiple waves of infection). The simulations suggest that fear-based home isolation at moderate levels (less than 50%) can have an impact on breaking transmission paths; however, its impact on the social contact network is highly sensitive to the duration that this intervention is in effect.

Our simulations show that if 100% of the schools close when 0.1% of the population is ill and they remain closed for the duration of the pandemic, the clinical attack rate could be reduced by more than 50%, when compared with the baseline. However, if schools reopen before the pandemic is over, a second wave is likely to appear and increase morbidity and mortality; thus, the parameters associated to a school closing policy should depend on the actual pandemic profile. For example, our results suggest that a temporary school closure policy may not be successful in

the sense that secondary waves of infection could be triggered if the school closure policy is suspended when the pandemic is still running its course.

The appearance of a second wave may imply a failed intervention strategy [41]; however, our results suggest that the overall clinical attack rate when a school closure intervention strategy is implemented is still lower than that obtained from the baseline scenario. Temporary school closures may have benefits beyond reducing morbidity and mortality, such as maintaining health-care services by spreading the number of hospitalizations over two waves. However, school closures indirectly contribute to absenteeism when parents must miss work to care for their children at home. Therefore, recommendations on school closures must be planned in advance to reduce the social and economic impact of absenteeism.

Fear-based home isolation can be effective in reducing morbidity and mortality and slowing transmission. The effectiveness of fear-based home isolation is determined by the fraction of the population that voluntarily withdraws from their daily activities for a week or two. We showed that as the number of people isolating at home increases, the clinical attack rate decreases. However, when the fraction of people self-isolating is over 50% (e.g., the intervention is too strong [26]) a second infection wave appears if home isolation is relaxed, leading to a larger clinical attack rate. It may not be feasible in reality for a large fraction of the population to self-isolate for a week or two; however, even if a small fraction of the population self-isolates, it can have a dramatic impact on reducing morbidity and mortality.

One of the most striking results of our study is the fact that temporary behavioral modifications have the potential to generate waves. This result raises an interesting question about the role that behavioral changes played in previous pandemics, since there were some temporary public health measures during the 1918 pandemic [6, 7, 12, 27]. There is a potential for multiple infection waves if public health measures are relaxed before the epidemic is over. Perhaps the most illustrative example of secondary waves is the 2002–2003 SARS epidemic in Toronto, Canada, where a secondary wave of infection occurred following a relaxation of infection-control precautions that were also associated with temporary increases in nosocomial transmission events [41]. The potential role that behavior changes may have played on the multiple wave pandemic profile observed during the 1918–1919 influenza pandemic in many regions of the world should not be discarded [6, 12, 27].

Early detection of index cases and early dissemination of information to the public are critical to empowering the population to make rational decisions, such as self-isolation. Capturing human behavior can have a profound influence in the predictions of future disease spread and the resources needed to contain an outbreak [19]. Modeling studies such as the one presented here could prove useful in providing estimates of the effects of changes in human behavior for future pandemic guidelines.

Acknowledgments We would like to acknowledge the Institutional Computing Program at Los Alamos National Laboratory for use of their HPC cluster resources. This research has

been supported at Los Alamos National Laboratory under the Department of Energy contract DE-AC52-06NA25396 and a grant from NIH/NIGMS in the Models of Infectious Disease Agent Study (MIDAS) program (U01-GM097658-01).

References

1. Ackerman, E., Elveback, L.R., Fox, J.P.: Simulation of Infectious Disease Epidemics. CC Thomas, Springfield, Illinois (1988)
2. Anderson, R.M., May, R.M.: Infectious Diseases of Humans. Oxford University Press, Oxford (1991)
3. Bansal, S., Pourbohloul, B., Meyers, L.A.: PLoS Med. e387 (2006)
4. Bansal, S., Grenfell, B.T., Meyers, L.A.: J. R. Soc. Interface **4**, 879 (2007)
5. Blower, S.M., Porco, T.C., Darby, G.: Nature Med. **4**, 673 (1998). doi: 10.1038/nm0698-673
6. Bootsma, M.C.J., Ferguson, N.M.: Proc. Natl. Acad. Sci. USA **104**, 7588 (2007). doi: 10.1073/pnas.0611071104
7. Caley, P., Philp, D.J., McCracken, K.: J. R. Soc. Interface **6**, 631 (2008). doi: 10.1098/rsif.2007.1197
8. Cauchemez, S., Valleron, A.J., Boëelle, P.Y., Flahault, A., Ferguson, N.M.: Nature **452**, 750 (2008). doi: 10.1038/nature06732
9. Centers for Disease Control and Prevention (CDC). Interim pre-pandemic planning guidance: Community strategy for pandemic influenza mitigation in the United States Early, targeted, layered use of nonpharmaceutical interventions. http://www.flu.gov/planning-preparedness/community/community_mitigation.pdf. Cited 4 Apr 2012
10. Chowell, G., Nishiura, H.: Phys. Life Rev. **5**, 50 (2008). doi: 10.1016/j.plrev.2007.12.001
11. Chowell, G., Hyman, J.M., Eubank, S., Castillo-Chavez, C.: Phys. Rev. E 68(6 Pt 2), 066102 (2003). doi: 10.1103/PhysRevE.68.066102
12. Chowell, G., Ammon, C.E., Hengartner, N.W., Hyman, J.M.: J. Theor. Biol. **241**, 193 (2006). doi: 10.1016/j.jtbi.2005.11.026
13. Colizza, V., Barrat, A., Barthelemy, M., Valleron, A., Vespignani, A.: PLoS Med. **4**, e13 (2007). doi: 10.1371/journal.pmed.0040013
14. Cooper, B.S., Pitman, R.J., Edmunds, W.J., Gay, N.J.: PLoS Med. **3**, e212 (2006). doi: 10.1371/journal.pmed.0030212
15. Del Valle, S., Hethcote, H., Hyman, J.M., Castillo-Chavez, C.: Math. Biosc. **195**, 228 (2005). doi: 10.1016/j.mbs.2005.03.006
16. Del Valle, S.Y., Hyman, J.M., Hethcote, H.W., Eugank, S.G.: Soc. Networks **29**, 539 (2007). doi: 10.1016/j.socnet.2007.04.005
17. Edmunds, W.J., O' Calaghan, C.J., Nokes, D.J.: Proc. R. Soc. B **22**, 264 (1997). doi: 10.1098/rspb.1997.0131
18. Eubank, S.G., Guclu, H., Kumar, V.A., Marathe, M.V., Srinivasan, A., Toroczkai, Z., Wang, N.: Nature **429**, 180 (2004). doi: 10.1038/nature02541
19. Ferguson, N.: Nature **446**, 733 (2007). doi: 10.1038/446733a
20. Ferguson, N.M., Keeling, M.J., Edmunds, W.J., Gani, R., Grenfell, B.T., Anderson, R.M., Leach, S.: Nature **425**, 681 (2003). doi:10.1038/nature02007
21. Ferguson, N.M., Cummings, D.A., Cauchemez, S., Fraser, C., Riley, S., Meeyai, A., Iamsirithaworn, S., Burke, D.S.: Nature **437**, 209 (2005). doi: 10.1145/1315843.1315857
22. Fukś, H., Lawniczak, A.T., Duchesne, R.: Eur. Phys. J. B **50**, 209 (2006). doi: 10.1140/epjb/e2006-00136-7
23. Gani, R., Hughes, H., Fleming, D., Griffin, T., Medlock, J., Leach, S.: Infect. Dis. **11**, 1355–1362 (2005)
24. Germann, T.C., Kadau, K., Longini, I.M. Jr., Macken, C.A.: Proc. Natl. Acad. Sci. USA **103**, 5935 (2006). doi: 10.1073/pnas.0601266103

25. Glass, K., Barnes, B.: Epidemiology **18**, 623 (2007). doi: 10.1097/EDE.0b013e31812713b4
26. Handel, A., Longini, I.M., Antia, R.: Proc. R. Soc. B **274**, 833 (2007). doi: 10.1098/rspb.2006.0015
27. Hatchett, R.J., Mecher, C.E., Lipsitch, M.: Proc. Natl. Acad. Sci. USA **104**, 7582 (2007). doi: 10.1073/pnas.0610941104
28. Hethcote, H.W.: SIAM Rev. **42**, 599 (2000). 10.1137/S0036144500371907
29. Isham, V., Mdley, G.: Models for Infectious Human Diseases: Their Structure and Relation to Data. Cambridge University Press, Cambridge (1996)
30. Johnson, N.P., Mueller, J.: Bull. Hist. Med. **76**, 105 (2002). doi: 10.1353/bhm.2002.0022
31. Kermack, W.O., McKendrick, A.G.: Proc. R. Soc. Series A **115**, 700 (1927). 10.1098/rspa.1927.0118
32. Kilbourne, E.D.: Emerg. Infec. Dis. **12**, 9 (2006). doi: 10.3201/eid1201.051254
33. Lin, J., Zhang, J., Dong, X., Fang, H., Chen, J., Su, N., Gao, Q., Zhang, Z., Liu, Y., Wang, Z., Yang, M., Sun, R., Li, C., Lin, S., Ji, M., Liu, Y., Wang, X., John, W., Feng, Z., Wang, Y., Yin, W.: Lancet **368**, 991 (2006). doi: 10.1016/S0140-6736(06)69294-5
34. Longini, I.M., Halloran, M.E., Nizam, A., Yang, Y.: Am. J. Epidemiol. **159**, 623 (2004). doi: 10.1093/aje/kwh092
35. Meyers, L.A., Pourbohloul, B., Newman, M.E.J., Skowronski, D.M., Brunham, R.C.: J. Theor. Biol. **232**, 71 (2004). doi: 10.1016/j.jtbi.2004.07.026
36. Michaels, J.: Commercial buildings energy consumption survey. (2003). http://www.eia.doe.gov/emeu/cbecs/cbecs2003/detailed_tables_2003/detailed_tables_2003.html. Cited 12 June 2012
37. National Household Travel Survey (NHTS). http://www.bts.gov/programs/national-household-travel-survey. Cited 4 April 2012
38. Neuzil, K.M., Hohlbein, C., Zhu, Y.: Arch. Pediar. Adolesc. Med. **156**, 986 (2002)
39. Newman, M.E.J.: Phys. Rev. E **66**, 016128 (2002). doi: 10.1103/PhysRevE.66.016128
40. Nuno, M., Chowell, G., Gumel, A.: J. R. Soc. Interface **22**, 505 (2007). doi: 10.1098/?rsif.2006.0186
41. Ofner-Agostini, M., Wallington, T., Henry, B., Low, D., McDonald, L.C., Berger, L., Mederski, B., SARS Investigative Team, Wong, T.: Investigation of the second wave (phase 2) of severe acute respiratory syndrome (SARS) in Toronto, Canada. What happened? Can. Commun. Dis. Rep. **34**, 1–11 (2008)
42. Pang, X., Zhu, Z., Xu, F., Guo, J., Gong, X., Liu, D., Liu, Z., Chin, D.P., Feikin, D.R.: J. Am. Med. Assoc. **290**, 3215 (2003)
43. Reed, J.M., Keeling, M.J.: Proc. R. Soc. B **270**, 699 (2003). doi: 10.1098/rspb.2002.2305
44. Ross, R.: The Prevention of Malaria. John Murray, London (1911)
45. Smith, D.J., Forrest, S., Ackley, D.H., Perelson, A.S.: Proc. Natl. Acad. Sci. USA **96**, 14001 (1999). doi: 10.1073/pnas.96.24.14001
46. Stilianakis, N.I., Perelson, A.S., Hayden F.G.: J. Infect. Dis. **177**, 863 (1998). doi: 10.1086/515246
47. Stohr, K., Esveld, M.: Science **306**, 2195 (2004). doi: 10.1126/science.1108165
48. Stroud, P.D., Del Valle, S.Y., Sydoriak, S.J., Riese, J., Mniszewski, S.: J. Artif. Soc. Soc. Simulat. **10**(4), 9 (2007)
49. US Homeland Security Council (HSC), National Strategy for Pandemic Influenza Implementation Plan. http://www.flu.gov/planning-preparedness/federal/pandemic-influenza-oneyear.pdf. Cited 4 Apr 2012
50. United Nations (UN), Department of Economic and Social Affairs, Population Division, Urban Population Development and the Environment (2007), http://www.un.org/esa/population/publications/2007-PopDevt/2007-PopDevt-Urban.htm. Cited 4 Apr 2012
51. Wallinga, J., Teunis, P., Kretzschmar, M.: Am. J. Epidemiol. **164**, 936 (2006). doi: 10.1093/aje/kwj317

52. Woodson, G.: 2005 Preparing for the Coming Influenza Pandemic. http://earthsky.org/health/grattan-woodson-interview Cited 4 Apr 2012
53. Yee, D., Bradford, J.: Employment density study, Canadian METRO Council Technical Report (1999)
54. Zaric, G.S.: Healthcare Manage. Sci. **5**, 147 (2002). doi: 10.1023/A:1014489218178